



OPEN

# Discovery of a selective, state-independent inhibitor of Na<sub>v</sub>1.7 by modification of guanidinium toxins

H. Pajouhesh<sup>1,6</sup>, J. T. Beckley<sup>2,6</sup>, A. Delwig<sup>1,6</sup>, H. S. Hajare<sup>3</sup>, G. Luu<sup>1</sup>, D. Monteleone<sup>1</sup>, X. Zhou<sup>1</sup>, J. Ligutti<sup>4</sup>, S. Amagasu<sup>4</sup>, B. D. Moyer<sup>4</sup>, D. C. Yeomans<sup>5</sup>, J. Du Bois<sup>3</sup> & J. V. Mulcahy<sup>1</sup>✉

The voltage-gated sodium channel isoform Na<sub>v</sub>1.7 is highly expressed in dorsal root ganglion neurons and is obligatory for nociceptive signal transmission. Genetic gain-of-function and loss-of-function Na<sub>v</sub>1.7 mutations have been identified in select individuals, and are associated with episodic extreme pain disorders and insensitivity to pain, respectively. These findings implicate Na<sub>v</sub>1.7 as a key pharmacotherapeutic target for the treatment of pain. While several small molecules targeting Na<sub>v</sub>1.7 have been advanced to clinical development, no Na<sub>v</sub>1.7-selective compound has shown convincing efficacy in clinical pain applications. Here we describe the discovery and characterization of ST-2262, a Na<sub>v</sub>1.7 inhibitor that blocks the extracellular vestibule of the channel with an IC<sub>50</sub> of 72 nM and greater than 200-fold selectivity over off-target sodium channel isoforms, Na<sub>v</sub>1.1–1.6 and Na<sub>v</sub>1.8. In contrast to other Na<sub>v</sub>1.7 inhibitors that preferentially inhibit the inactivated state of the channel, ST-2262 is equipotent in a protocol that favors the resting state of the channel, a protocol that favors the inactivated state, and a high frequency protocol. In a non-human primate study, animals treated with ST-2262 exhibited reduced sensitivity to noxious heat. These findings establish the extracellular vestibule of the sodium channel as a viable receptor site for the design of selective ligands targeting Na<sub>v</sub>1.7.

The voltage-gated sodium ion channel (Na<sub>v</sub>) isoform 1.7 has emerged as a high-interest target for the discovery of non-opioid pain therapeutics based on compelling validation from human genetics and preclinical studies<sup>1</sup>. Na<sub>v</sub>1.7 loss-of-function mutations result in whole-body insensitivity to pain; conversely, gain-of-function variants are associated with episodic extreme pain disorders and small fiber neuropathies<sup>2–5</sup>. Discovery of selective inhibitors of Na<sub>v</sub>1.7 has been challenging due to the structural conservation of off-target Na<sub>v</sub> isoforms (Na<sub>v</sub>1.1–1.6, Na<sub>v</sub>1.8 and Na<sub>v</sub>1.9), inhibition of which is likely to result in safety liabilities<sup>6–8</sup>.

Na<sub>v</sub>s are integral membrane proteins expressed in excitable cells that comprise a ~260 kD pore-forming α-subunit and up to two accessory β-subunits (Fig. 1A)<sup>9</sup>. The central pore of the α-subunit is encircled by four voltage-sensing domains (VSD I–IV). Channel gating occurs through protein conformational changes in response to membrane depolarization. At least nine discrete binding sites on the Na<sub>v</sub> α-subunit have been identified for peptides and small molecules that influence ion conductance<sup>10</sup>. The large majority of molecules that engage Na<sub>v</sub>s bind preferentially to a specific conformational state of the channel and show use-dependent activity. Clinical Na<sub>v</sub> inhibitors (e.g., bupivacaine, lidocaine, carbamazepine) are both state- and frequency-dependent agents that lodge in the intracellular pore of the α-subunit, a site that is highly conserved between isoforms. These drugs rely on local administration to achieve a margin between the desired pharmacodynamic effect and dose-limiting side effects. Certain investigational Na<sub>v</sub> inhibitors, such as peptide toxins isolated from venomous species, interact with VSDs to alter the kinetics or voltage dependence of channel activation or inactivation<sup>11,12</sup>. Similarly, a class of small molecule aryl and acyl sulfonamide compounds bind to an activated conformation of VSD IV and prevent

<sup>1</sup>SiteOne Therapeutics, South San Francisco, CA 94080, USA. <sup>2</sup>SiteOne Therapeutics, Bozeman, MT 59715, USA. <sup>3</sup>Department of Chemistry, Stanford University, Stanford, CA 94305, USA. <sup>4</sup>Neuroscience Department, Amgen Research, Thousand Oaks, CA 91320, USA. <sup>5</sup>Department of Anesthesiology, Perioperative, and Pain Medicine, Stanford University, Stanford, CA 94305, USA. <sup>6</sup>These authors contributed equally: H. Pajouhesh, J. T. Beckley and A. Delwig. ✉email: john.mulcahy@site1therapeutics.com

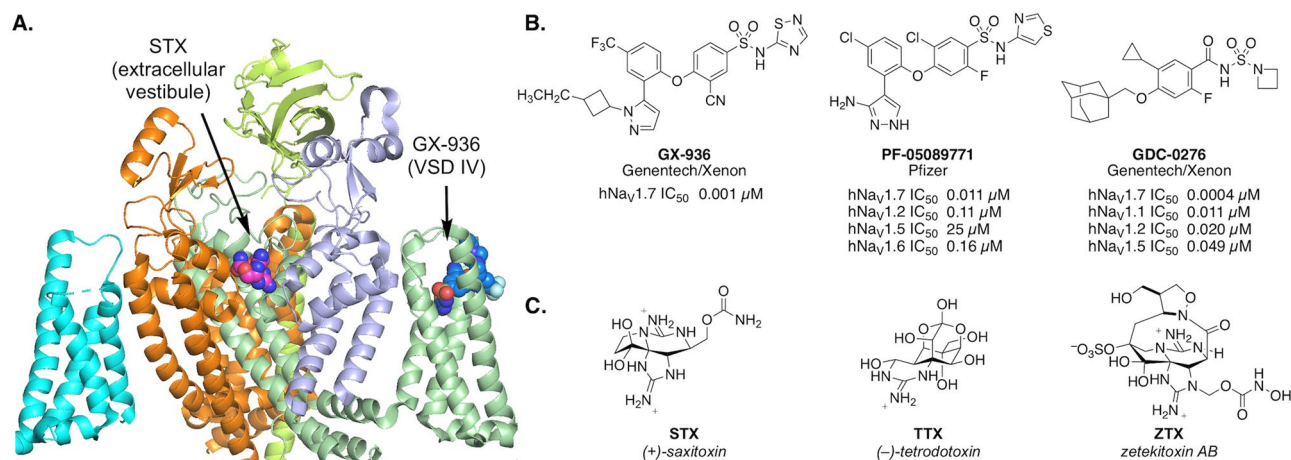


**Figure 1.** (A) Cryo-EM structure of STX bound to human Na<sub>v</sub>1.7-β1-β2 complex (PDB: 6j8g) with GX-936 positioned approximately based on PDB: 5ek0 in Pymol version 2.0.4 (Schrodinger, New York, NY). (B) Representative Na<sub>v</sub>1.7 inhibitors that bind VSD IV. (C) Natural Na<sub>v</sub> inhibitors that bind to the extracellular vestibule<sup>18–21</sup>.

recovery from inactivation (Fig. 1B)<sup>13–16</sup>. By contrast, cationic guanidinium toxins and peptide cone snail toxins inhibit ion conduction by sterically occluding the extracellular vestibule of the channel pore (Site 1). The former are a unique collection of small molecule natural products exemplified by saxitoxin and tetrodotoxin—high affinity, state-independent blockers against six of nine Na<sub>v</sub> subtypes (Fig. 1C)<sup>17</sup>.

In the pursuit of isoform-selective inhibitors of Na<sub>v</sub>1.7, two binding sites, the cystine knot toxin site at VSD II and the sulfonamide site at VSD IV, have been heavily interrogated. Certain cystine knot toxins that engage VSD II such as HwTx-IV, Pn3a, and ProTx-II exhibit 6–1,000× selectivity for Na<sub>v</sub>1.7 over other channel isoforms. Potency and selectivity for this target have been improved with synthetic peptide toxin derivatives<sup>22–26</sup>. Among small, Lipinski-type molecules, only the aryl and acyl sulfonamides pioneered by Icagen/Pfizer and subsequently investigated by Amgen, Chromocell, Genentech/Xenon, Merck, and others have shown evidence of significant Na<sub>v</sub>1.7 isoform selectivity<sup>7,16</sup>. Within the sulfonamide series, selectivity levels are > 1,000× over certain off-target isoforms including the cardiac isoform, Na<sub>v</sub>1.5, but generally 10–50× against Na<sub>v</sub>1.2 and Na<sub>v</sub>1.6. Many but not all sulfonamide Na<sub>v</sub>1.7 inhibitors suffer from undesirable pharmaceutical properties, including high plasma protein binding (e.g. > 99.8%), cytochrome p450 inhibition, in vitro hepatotoxicity and high unbound clearance<sup>27,28</sup>, which have hindered clinical development. Although a number of candidates have been advanced to human testing, one compound has been discontinued after a Phase 2 study likely due to limited efficacy (PF-05089771); others have been discontinued after Phase 1 trials for reasons that may be related to safety liabilities such as elevated expression of liver transaminases and hypotension (GDC-0276)<sup>29,30</sup>.

Electrophysiology studies with naturally occurring Site 1 ligands against different wild-type and mutant Na<sub>v</sub> isoforms have identified the extracellular vestibule of Na<sub>v</sub>1.7 as a promising locus for selective inhibitor design<sup>31–33</sup>. The outer mouth of the channel is formed from residues that link the S5–S6 helices (referred to as pore loops) from each of the four domains. The domain III pore loop of human Na<sub>v</sub>1.7 contains a T1398/I1399 sequence motif that is not present in other human Na<sub>v</sub> subtypes (which contain MD at equivalent positions, Suppl Table 1)<sup>31</sup>. Comparison of the amino acid sequence of the domain III pore loop across species indicates that the sequence motif in hNa<sub>v</sub>1.7 is unique to primates. The half-maximal inhibitory concentration (IC<sub>50</sub>) value for saxitoxin (STX) is markedly altered (250-fold change) depending on the presence or absence of the T1398 and I1399 residues. Against rNa<sub>v</sub>1.4, the IC<sub>50</sub> of STX is 2.8 ± 0.1 nM compared to 702 ± 53 nM for hNa<sub>v</sub>1.7<sup>31</sup>. Introduction of the alternative domain III pore loop sequence by mutagenesis restores potency (hNa<sub>v</sub>1.7 T1398M/I1399D IC<sub>50</sub> = 2.3 ± 0.2 nM). These findings suggest that it may be possible to capitalize on structural differences in the extracellular vestibule between hNa<sub>v</sub> isoforms to design Na<sub>v</sub>1.7-selective inhibitors.

Recent advances in the de novo synthesis of guanidinium toxin analogues have enabled systemic examination of the structure–activity relationship (SAR) properties that govern hNa<sub>v</sub>1.7 potency and isoform selectivity<sup>34–37</sup>. Prior to 2016, the binding orientation of STX proposed in the literature indicated that the C11 methylene carbon was positioned proximally to domain III pore loop residues<sup>38–40</sup>. SAR and mutant cycle analysis studies posited a revised pose in which the C13 carbamate moiety abuts DIII<sup>32</sup>. This revised binding pose was recently confirmed by cryoelectron microscopy (cryo-EM) structures of STX bound to Na<sub>v</sub>PaS and hNa<sub>v</sub>1.7<sup>18,41</sup>. In the present study, analogues of STX substituted at both the C11 and C13 positions were investigated to understand the requirements for selective inhibition of hNa<sub>v</sub>1.7. These efforts led to the discovery of ST-2262, a potent and selective inhibitor of Na<sub>v</sub>1.7 that reduces sensitivity to noxious heat in a preliminary study in non-human primates (NHPs).

## Results

**Discovery of ST-2262.** ST-2262 was discovered through a rational design strategy aimed at identifying derivatives of natural bis-guanidinium toxins that preferentially inhibit hNa<sub>v</sub>1.7 over other off-target hNa<sub>v</sub> isoforms<sup>31</sup>. Mutagenesis, homology modeling, and docking studies conducted prior to 2016 suggested that bis-

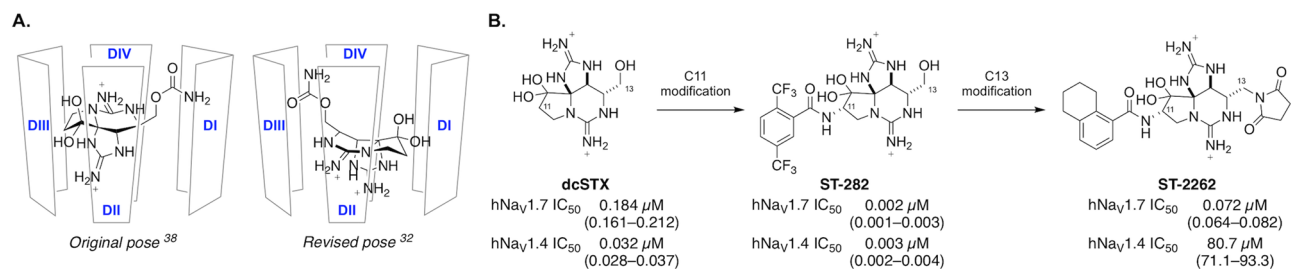


**Figure 2.** (A) The consensus pose for binding of STX in the extracellular vestibule of Na<sub>v</sub> oriented C11 in proximity to the DIII pore loop prior to 2016<sup>38</sup>. A revised pose based on mutant cycle analysis and recent cryo-EM structures orients the C13 carbamate near DIII<sup>32,41</sup>. (B) ST-2262 was discovered by a rational design strategy aimed at identifying functional groups that interact with the DIII T1398/I1399 sequence motif unique to primate Na<sub>v</sub>1.7. Values are mean (95% CI).

guanidinium toxins orient in the outer mouth of the channel with the C11 methylene center positioned toward the domain III pore loop of Na<sub>v</sub> (Fig. 2A, Original pose)<sup>38–40</sup>. Exploration of substitution at C11 of decarbamoyl saxitoxin (dcSTX) led to the identification of a series of analogues bearing aryl amide groups at this site. Certain compounds, as exemplified by ST-282, show excellent potency against hNa<sub>v</sub>1.7 but minimal selectivity (~1:1) over off-target isoforms such as hNa<sub>v</sub>1.4 (Fig. 2B). The finding that hNa<sub>v</sub>1.7 isoform selectivity could not be achieved by modification of the C11 substituent led us to investigate SAR at alternative positions. These studies followed evidence that the proper binding orientation of STX is rotated ~180° from earlier models, thus placing the C13 substituent in close proximity to domain III (Fig. 2A, Revised pose)<sup>32</sup>.

Derivatives of STX bearing amide, carbamate, ester, ether, and urethane substituents at the C13 position were prepared in an effort to identify compounds with improved selectivity for hNa<sub>v</sub>1.7. Insight from studies of a naturally-occurring STX C13 acetate congener, STX-OAc, helped guide selection of compounds for synthesis (Suppl Figure 1)<sup>32</sup>. The difference in potencies between STX and STX-OAc is striking considering that these two structures vary at a single position (NH<sub>2</sub> → CH<sub>3</sub>). Following this lead, we explored substituents at C13 that could replace the hydrolytically unstable acetate group. Ultimately, the C13 succinimide was discovered as a suitable acetate isostere, which was paired with a C11 tetrahydronaphthyl amide to generate ST-2262, the focus of the present study.

**ST-2262 is a potent and selective inhibitor of hNa<sub>v</sub>1.7.** The potency of ST-2262 against hNa<sub>v</sub>1.7 stably expressed in HEK293 cells was assessed by manual patch clamp electrophysiology with a voltage-protocol that favors the resting state of the channel. Using a stimulation protocol with a holding potential of -110 mV and a stimulus frequency of 0.33 Hz, the IC<sub>50</sub> of ST-2262 against hNa<sub>v</sub>1.7 was measured at 0.072 μM (95% confidence interval (CI) 0.064–0.082) (Fig. 3A, Suppl Table 2). Potencies against off-target sodium channel isoforms (hNa<sub>v</sub>1.1–1.6, hNa<sub>v</sub>1.8) were determined following a similar protocol. Activity against hNa<sub>v</sub>1.9 was not evaluated due to the difficulty of expressing this subtype heterologously<sup>42</sup>. ST-2262 was determined to be >200-fold selective over hNa<sub>v</sub>1.6 (IC<sub>50</sub> = 17.9 μM, 95% CI 14.8–22.1), >900-fold selective over hNa<sub>v</sub>1.3 (IC<sub>50</sub> = 65.3 μM, CI 62.7–68.1), and >1,000-fold selective over all other Na<sub>v</sub> isoforms tested. Similar IC<sub>50</sub> values against the eight hNa<sub>v</sub> subtypes were obtained in an independent study using the PatchXpress automated electrophysiology platform (Suppl Table 3).

Exposure of hNa<sub>v</sub>1.1 and hNa<sub>v</sub>1.2 to high concentrations of ST-2262 (10–100 μM) resulted in a reduction of the rate of fast inactivation; a similar effect was noted, albeit to a lesser degree, with hNa<sub>v</sub>1.3 and hNa<sub>v</sub>1.4 (Suppl Figure 2). Lower concentrations of ST-2262 (1–3 μM), which remain sufficiently high to achieve >90% inhibition of hNa<sub>v</sub>1.7, had no measurable effect on fast inactivation of hNa<sub>v</sub>1.1 and hNa<sub>v</sub>1.2. It is possible that elevated concentrations of ST-2262 result in a secondary mode of binding against these Na<sub>v</sub> subtypes, however, efforts have not been made to examine such a mechanism at this time. To our knowledge, changes in the rate of fast inactivation have not been observed with STX.

To investigate whether the potency of ST-2262 was dependent on the membrane holding potential or frequency of stimulus, an IC<sub>50</sub> value was measured against hNa<sub>v</sub>1.7 using a two-pulse protocol with a pre-pulse to the voltage at half-inactivation (8 s step) and with a protocol that depolarizes the cell at high frequency (30 Hz stimulus). The potency of ST-2262 was not appreciably altered using either stimulation protocol (IC<sub>50</sub> = 0.087 μM, 0.056–0.120 and IC<sub>50</sub> = 0.112 μM, 0.015–0.357, respectively; Fig. 3B, Suppl Table 4). These results indicate that ST-2262 is a selective, use-independent inhibitor of hNa<sub>v</sub>1.7.

**Species variation in potency and mutagenesis.** The potency of ST-2262 was assessed against a panel of species variants of Na<sub>v</sub>1.7, including mouse, rat, and cynomolgus monkey (Suppl Table 5). Consistent with the hypothesis that Na<sub>v</sub>1.7 potency is affected by the presence of the T1398/I1399 sequence motif in the DIII pore loop, the IC<sub>50</sub> of ST-2262 against cynoNa<sub>v</sub>1.7 (0.101 μM, 0.073–0.140) was similar to human. In contrast, ST-2262 was >50× less potent against mouse (IC<sub>50</sub> = 3.78 μM, 3.23–4.43) and rat Na<sub>v</sub>1.7 (IC<sub>50</sub> = 4.95 μM, 4.17–5.87) than the human ortholog. Affinity was restored within twofold of the hNa<sub>v</sub>1.7 potency by introduction of domain III MD-TI mutations to mouse Na<sub>v</sub>1.7 (IC<sub>50</sub> = 0.130 μM, 0.055–0.307; Fig. 3C, Suppl Table 6).

Multiple lines of evidence suggest that ST-2262 binds to the extracellular vestibule of the sodium channel (i.e., Site 1) including: (i) the structural similarity of ST-2262 to natural bis-guanidinium toxin ligands, (ii) the

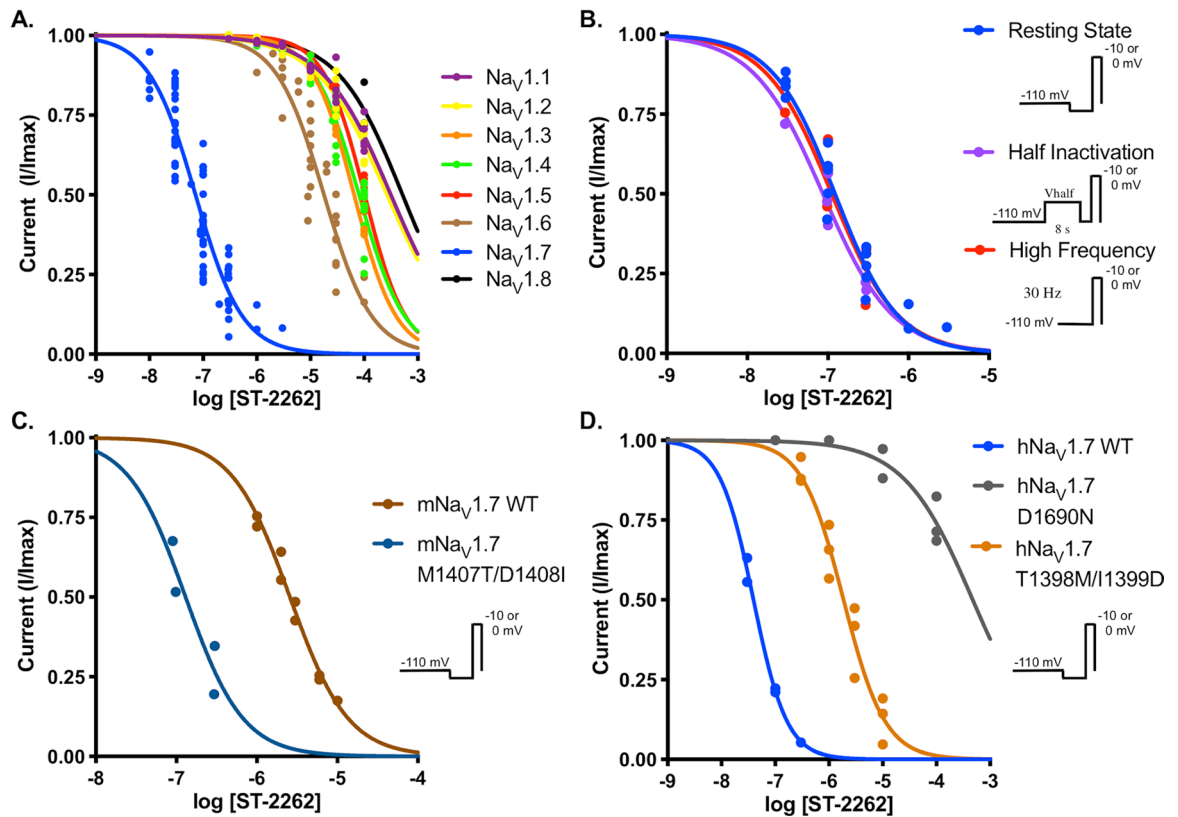


**Figure 3.** (A) Dose–response curves for the inhibitory effect of ST-2262 on  $\text{Na}_V1.1$ – $\text{Na}_V1.8$  stably expressed in CHO or HEK293 cells using a single-pulse (resting state) protocol with a 10 ms pulse from a holding potential of  $-110$  mV to voltage at peak activation ( $-20$  to  $+10$  mV).  $\text{Na}_V1.X$   $\text{IC}_{50}$  (in  $\mu\text{M}$ , mean, 95% CI).  $\text{Na}_V1.1$ :  $> 100$ ;  $\text{Na}_V1.2$ :  $> 100$ ;  $\text{Na}_V1.3$ : 65.3, 62.7–68.1;  $\text{Na}_V1.4$ : 80.7, 71.1–93.3;  $\text{Na}_V1.5$ :  $> 100$ ;  $\text{Na}_V1.6$ : 17.9, 14.8–22.1;  $\text{Na}_V1.7$ : 0.072, 0.064–0.082;  $\text{Na}_V1.8$ :  $> 100$ . (B) Comparison of dose–response relationship of ST-2262 inhibition against  $\text{Na}_V1.7$  using different stimulation protocols: resting state; two-pulse protocol contained an 8 s conditioning step to the voltage at half-inactivation, followed by a 20 ms step to voltage at full activation (half-inactivation protocol)<sup>16</sup>; high frequency single-pulse protocol stimulated at 30 Hz.  $\text{Na}_V1.7$   $\text{IC}_{50}$  (in  $\mu\text{M}$ , mean, 95% CI). Resting state: 0.123, 0.104–0.145; half-inactivation: 0.087, 0.056–0.120; high frequency: 0.112, 0.015–0.357. (C) Comparison of dose–response relationship of  $\text{Na}_V1.7$  inhibition against WT  $\text{mNa}_V1.7$  and M1407T/D1408I  $\text{mNa}_V1.7$  on a resting state protocol.  $\text{mNa}_V1.7$   $\text{IC}_{50}$  (in  $\mu\text{M}$ , 95% CI). WT: 2.57, 2.30–2.87; M1407T/D1408I: 0.130, 0.055–0.307. (D) Comparison of dose–response of ST-2262 against transiently expressed  $\text{hNa}_V1.7$  WT,  $\text{hNa}_V1.7$  D1690N, and  $\text{hNa}_V1.7$  T1398M/I1399D.  $\text{IC}_{50}$  (in  $\mu\text{M}$ , mean, 95% CI). WT: 0.039, 0.032–0.047; D1690N:  $> 100$ ; T1398M/I1399D: 1.87, 1.47–2.39.

state- and frequency-independent mode of  $\text{Na}_V$  inhibition that is characteristic of extracellular pore blockers, and (iii) the influence of DIII pore loop residues on potency. To gain additional support that ST-2262 binds to the outer pore of  $\text{Na}_V$ , we generated a point mutant of  $\text{hNa}_V1.7$ , D1690N, at a position known to significantly destabilize binding of STX<sup>39</sup>. The domain IV residue D1690 forms a critical bridged hydrogen bond with the C12 hydrated ketone of STX<sup>39,41</sup>. We also measured potency against the  $\text{hNa}_V1.7$  T1398M/I1399D double mutant to directly confirm that the domain III TI sequence motif contributes to  $\text{hNa}_V1.7$  affinity<sup>31</sup>. The introduction of other point mutations to  $\text{Na}_V1.7$  was attempted (Y362S and E916A), but these variants proved challenging to express<sup>39,43</sup>. ST-2262 exhibited a  $> 1,000$ -fold loss in potency against  $\text{hNa}_V1.7$  D1690N ( $\text{IC}_{50} > 100 \mu\text{M}$ ) and a  $\sim 48$ -fold loss against  $\text{hNa}_V1.7$  T1398M/I1399D ( $\text{IC}_{50} = 1.87 \mu\text{M}$ , 1.47–2.39) compared to the wild-type channel ( $\text{IC}_{50} = 0.039 \mu\text{M}$ , 0.032–0.047; Fig. 3D, Suppl Table 6). Collectively, these results indicate that ST-2262 binds to the extracellular vestibule of  $\text{Na}_V1.7$ , displaying significant species variation in potency and isoform selectivity in large part due to molecular interactions with residues T1398 and I1399, which are unique to human and non-human primate  $\text{Na}_V1.7$  orthologs<sup>31,32</sup>.

**ST-2262 increases withdrawal latency in a nonhuman primate model of thermal pain.** Mice and humans with genetic  $\text{Na}_V1.7$  loss-of-function are profoundly insensitive to noxious heat<sup>2,3,44–46</sup>. To understand whether pharmacological block of  $\text{Na}_V1.7$  affects noxious thermal sensitivity, we conducted an initial evaluation ( $n = 4$ ) of the effect of ST-2262 in a non-human primate (NHP) model of acute thermal pain. Experiments were approved by the Montana State University institutional animal care and use committee and performed in accordance with institutional, national, and international guidelines and regulations. It is not possible to study the influence of ST-2262 on acute thermal pain in rodents as this compound is  $> 50$ -fold less potent against

Na<sub>v</sub>1.7 in species that lack the T1398/I1399 sequence motif (Suppl Table 5). A NHP model of acute thermal pain was identified that uses a heat lamp to deliver a stimulus to the dorsal surface of the hand of lightly anesthetized cynomolgus macaques and measures the time to withdrawal<sup>47</sup>. Prior to advancing ST-2262 into the NHP acute thermal pain model, a standard battery of preclinical assays was completed to evaluate ADME and pharmacokinetic properties of this compound in cynomolgus macaques (Suppl Table 7). Off-target activity of ST-2262 using a commercially available radioligand binding assay panel against 68 different targets was also measured (LeadProfilingScreen, Eurofins, Taipei, Taiwan). No hits were identified on the off-target panel, defined as > 50% inhibition with 10 μM ST-2262 (Suppl Table 8).

Male cynomolgus monkeys were anesthetized with propofol to a level in which the withdrawal reflex of the hand occurred at a consistent latency of approximately 3 s, a response time that was comparable to the detection of sharp pain from Aδ fibers when tested in prior studies on human volunteers<sup>48,49</sup>. The dorsal surface of the hand was exposed to a thermal stimulus that selectively activates Aδ-fiber nociceptors (Fig. 4A–C)<sup>47,50</sup>. The thermal stimulus was turned off at 5 s to prevent tissue damage. Heart rate was monitored throughout the study, and presentation of the noxious thermal stimuli consistently led to a transient increase in heart rate that peaked seconds after the stimulus and then returned to baseline (ΔHR). Acute noxious thermal stimuli transiently increase heart rate in human subjects; the percent change in heart rate correlates with subjective pain score<sup>51</sup>.

ST-2262 hydrochloride administered IV increased the withdrawal latency to noxious thermal stimuli (Fig. 4A). Efficacy was assessed in one subject at four dose levels (0.01, 0.05, 0.25, 1.25 mg/kg), in two subjects at the three higher dose levels (0.05, 0.25, 1.25 mg/kg), and in one additional subject at the highest dose level only (1.25 mg/kg). At the highest dose of 1.25 mg/kg, all four animals showed no hand withdrawal prior to the 5 s cut-off latency (Fig. 4A), a significant increase in withdrawal latency compared to baseline values (Mixed effects model:  $F(3,7) = 7.468$ ,  $p < 0.05$ ; 0.01 mg/kg was not included in this analysis because only one subject received this dose). The 1.25 mg/kg dose of ST-2262 also almost completely reduced ΔHR (Fig. 4B; Mixed effects model:  $F(3,7) = 6.654$ ,  $p < 0.05$ ).

Plasma samples were obtained from animals to assess the PK/PD relationship between drug exposure and thermal withdrawal latency. We found that 0.25 mg/kg ST-2262 resulted in ~1,400 ng/ml in plasma at the 5 min time point ( $n = 2$ ), which corresponds to 7× the IC<sub>50</sub> value of ST-2262 against cynoNa<sub>v</sub>1.7, corrected for plasma protein binding (cyno PPB = 73.5%). The unbound exposure of drug was reduced to 3.4× cynoNa<sub>v</sub>1.7 IC<sub>50</sub> at the 30 min time point. At a dose of 1.25 mg/kg, the total plasma concentration was ~7,000 ng/ml at 5 min ( $n = 2$ ), which corresponds to an unbound exposure of 32× cynoNa<sub>v</sub>1.7 IC<sub>50</sub>, and was maintained above 15× cynoNa<sub>v</sub>1.7 IC<sub>50</sub> for over 100 min (Fig. 4C). Lumbar CSF samples collected from two animals receiving the 1.25 mg/kg dose indicated that ST-2262 was peripherally restricted, with CSF:plasma ratios < 10<sup>-3</sup> ( $n = 2$ ; [ST-2262] 0.8, < 0.5 ng/ml in CSF).

By adjusting radiant heat parameters, the noxious heat model can be used to selectively assess responses to cutaneous C-fiber nociceptor activation, which produces a burning pain in volunteers<sup>48,49</sup>. The effect of ST-2262 on C-fiber induced hand withdrawal and heart rate change was investigated on two cynomolgus subjects<sup>47</sup>. As with the Aδ nociceptive response, 1.25 mg/kg ST-2262 completely abolished the C-fiber-mediated hand withdrawal and ΔHR (Fig. 4D,E). Collectively, these results are consistent with the hypothesis that pharmacological block of Na<sub>v</sub>1.7 reduces sensitivity to noxious heat, phenotypically analogous to studies of Na<sub>v</sub>1.7 loss-of-function in CIP patients<sup>2</sup>. In addition, analysis of the PK/PD relationship of ST-2262 in this model provides insight into the level of Na<sub>v</sub>1.7 target occupancy that may be necessary to achieve a pharmacodynamic effect. Recognizing the limited number of animals tested due to the challenge of working with non-human primates, additional work is warranted to further define the relationship between pharmacological inhibition of Na<sub>v</sub>1.7 and sensitivity to noxious thermal stimuli.

## Discussion

The finding that humans lacking functional Na<sub>v</sub>1.7 exhibit an inability to experience pain raises the intriguing possibility that selective inhibitors of Na<sub>v</sub>1.7 may be potent analgesics<sup>1–3</sup>. In the present study, we describe the discovery and characterization of ST-2262, a selective pore blocker of hNa<sub>v</sub>1.7 advanced through rational modification of a natural small molecule toxin lead, STX. In whole cell voltage clamp recordings, ST-2262 exhibited > 200-fold selectivity for hNa<sub>v</sub>1.7 over hNa<sub>v</sub>1.1–1.6 and hNa<sub>v</sub>1.8. The selectivity of ST-2262 was not examined against hNa<sub>v</sub>1.9, a channel subtype that is difficult to express in heterologously. hNa<sub>v</sub>1.9 contains a residue in the domain I p-loop, S360, that confers resistance to STX and lacks the domain III threonine/isoleucine sequence motif that is essential for high potency of ST-2262 against hNa<sub>v</sub>1.7. Thus, inhibition of Na<sub>v</sub>1.9 by ST-2262 is unlikely<sup>42</sup>.

The properties of ST-2262 are in contrast to other preclinical and clinical inhibitors of Na<sub>v</sub>1.7, which preferentially bind to an inactivated conformation(s) of the channel<sup>52</sup>. Mutagenesis experiments indicate that specific residues in the extracellular pore of Na<sub>v</sub>1.7, including a two amino acid sequence variation in the domain III pore loop that is unique to primates, are required for ST-2262 binding to cyno- and human Na<sub>v</sub>1.7<sup>31,39</sup>. These findings establish the extracellular vestibule of Na<sub>v</sub>1.7 as a viable receptor site for the design of potent and selective channel inhibitors.

Whereas congenital insensitivity to pain in humans is the result of complete and permanent Na<sub>v</sub>1.7 loss-of-function, inhibition by small molecule agents is incomplete and transient. This difference raises several important questions regarding the pharmacology of Na<sub>v</sub>1.7: (1) is transient inhibition sufficient for analgesia, (2) what level of target engagement is required for efficacy, and (3) what anatomic compartment(s) must be accessed? In light of the preliminary nature of the behavioral studies conducted with ST-2262, the present study does not yield definitive answers to these questions. Nevertheless, the finding that NHPs administered ST-2262 exhibited reduced sensitivity to noxious thermal stimuli is consistent with the view that transient inhibition of Na<sub>v</sub>1.7

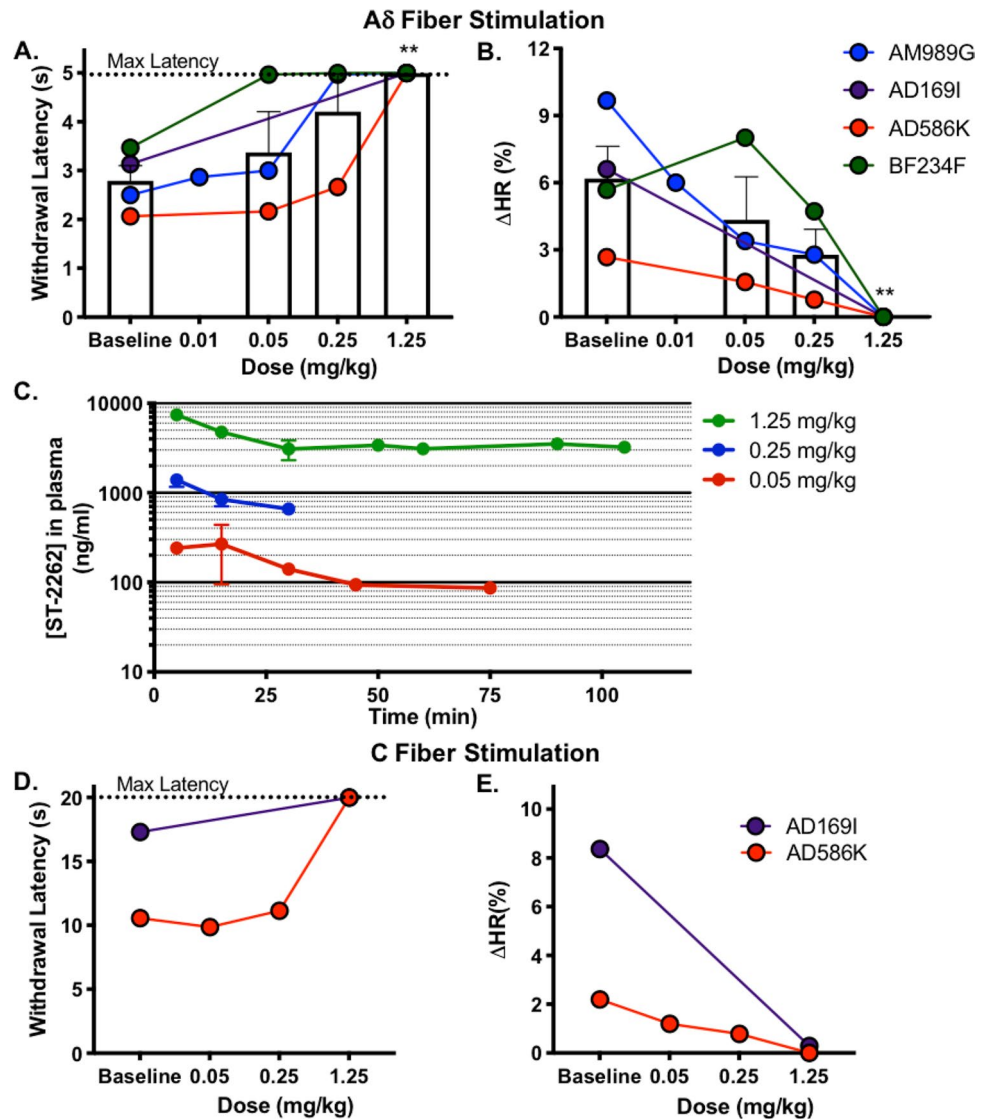


**Figure 4.** ST-2262 increases withdrawal latency and reduces thermal evoked heart rate increase in a non-human primate noxious heat model. (A,B) Individual subject data points showing changes in withdrawal latency (A) and transient change in heart rate ( $\Delta$ HR) (B) following thermal stimuli. Bar graphs are expressed as mean  $\pm$  SEM. \*\*Dunnett's multiple comparison test, compared to baseline,  $p < 0.01$ . (C) Plasma level concentration of ST-2262 in plasma at different doses. (D,E) A lower heating rate thermal stimulus was presented for a maximum of 20 s, which selectively activates C fibers<sup>47</sup>. In two subjects, the C-fiber-induced hand withdrawal response was replicable for testing. The efficacy endpoints measured were withdrawal latency (A) and heart rate change (B).

is sufficient to produce analgesia<sup>45</sup>. Furthermore, recognizing that ST-2262 is a polar small molecule with low membrane permeability and therefore unlikely to reach efficacious concentrations in the CNS (analysis of CSF samples obtained during NHP experiments gave a CSF:plasma ratio of  $< 10^{-3}$ ), the observed effects on thermal withdrawal latency and  $\Delta$ HR are likely the result of peripheral inhibition. Our findings, however, do not rule out an additional role for Na<sub>v</sub>1.7 at the central terminals of primary afferents or in dorsal horn neurons, as has been suggested<sup>53</sup>.

In the present study, the effect of ST-2262 on withdrawal latency to noxious heat was measured in NHPs at doses of 0.01, 0.05, 0.25 and 1.25 mg/kg IV. Doses of 0.05, 0.25 and 1.25 mg/kg resulted in unbound plasma concentrations of ST-2262 of 0.7 $\times$ , 3.4 $\times$  and 16 $\times$  the IC<sub>50</sub> value against cynoNa<sub>v</sub>1.7 at a time point 30 min following drug administration. Assuming a unitary Hill coefficient, which is consistent with the dose–response relationship for ST-2262 in whole cell recordings against cyno- and human Na<sub>v</sub>1.7, these unbound exposures correspond to 41%, 78% and 94% inhibition of Na<sub>v</sub>1.7, respectively. Further work to understand whether a similar relationship exists between Na<sub>v</sub>1.7 target occupancy and analgesic pharmacodynamic effects in other preclinical pain models is ongoing.

## Conclusion

Na<sub>v</sub>1.7 remains a compelling target for the development of non-opioid analgesics based on evidence from human genetics and rodent knock-out studies<sup>2,3,44,45</sup>. A major challenge in the pursuit of safe and effective Na<sub>v</sub>1.7 inhibitors has been the identification of small molecules that are selective over off-target proteins, including other Na<sub>v</sub> isoforms, to achieve a suitable margin of safety. Prior efforts to develop high precision Na<sub>v</sub>1.7 inhibitors have largely focused on a class of aryl and acyl sulfonamides that bind preferentially to VSD IV and impede recovery from inactivation<sup>7</sup>. In the present study, we disclose ST-2262, a synthetic analogue of natural bis-guanidinium toxins that lodges in the extracellular vestibule of the channel (Site 1) and occludes ion passage. A preliminary PK/PD study involving intravenous administration of ST-2262 to four cynomolgus subjects demonstrated increased withdrawal latency to noxious heat. Collectively, our findings validate the extracellular mouth of the sodium channel as a tractable receptor site for selective ligand design and provide insight into the distribution and target occupancy requirements for drug efficacy mediated by inhibition of Na<sub>v</sub>1.7.

## Data availability

Additional raw data are available from the corresponding author on reasonable request.

Received: 16 April 2020; Accepted: 6 August 2020

Published online: 09 September 2020

## References

- Dib-Hajj, S. D., Yang, Y., Black, J. A. & Waxman, S. G. The Na<sub>v</sub>1.7 sodium channel: From molecule to man. *Nat. Rev. Neurosci.* **14**, 49–62 (2013).
- Cox, J. J. *et al.* An SCN9A channelopathy causes congenital inability to experience pain. *Nature* **444**, 894–898 (2006).
- Goldberg, Y. *et al.* Loss-of-function mutations in the Nav1.7 gene underlie congenital indifference to pain in multiple human populations. *Clin. Genet.* **71**, 311–319 (2007).
- Yang, Y. *et al.* Mutations in SCN9A, encoding a sodium channel alpha subunit, in patients with primary erythralgia. *J. Med. Genet.* **41**, 171–174 (2004).
- Faber, C. G. *et al.* Gain of function Na<sub>v</sub>1.7 mutations in idiopathic small fiber neuropathy. *Ann. Neurol.* **71**, 26–39 (2012).
- Payandeh, J. & Hackos, D. H. Selective ligands and drug discovery targeting the voltage-gated sodium channel Nav1.7. In *Voltage-gated Sodium Channels: Structure, Function and Channelopathies*, Vol. 246 (ed. Chahine, M.) 271–306 (Springer International Publishing, Berlin, 2018).
- McKerrall, S. J. & Sutherlin, D. P. Nav1.7 inhibitors for the treatment of chronic pain. *Bioorg. Med. Chem. Lett.* **28**, 3141–3149 (2018).
- Mulcahy, J. V. *et al.* Challenges and opportunities for therapeutics targeting the voltage-gated sodium channel isoform Na<sub>v</sub>1.7. *J. Med. Chem.* <https://doi.org/10.1021/acs.jmedchem.8b01906> (2019).
- Ahern, C. A., Payandeh, J., Bosmans, F. & Chanda, B. The hitchhiker's guide to the voltage-gated sodium channel galaxy. *J. Gen. Physiol.* **147**, 1–24 (2016).
- Stevens, M., Peigneur, S. & Tytgat, J. Neurotoxins and their binding areas on voltage-gated sodium channels. *Front. Pharmacol.* **2**, 71 (2011).
- Israel, M. R., Tay, B., Deuis, J. R. & Vetter, I. Sodium channels and venom peptide pharmacology. In *Advances in Pharmacology*, vol. 79, 67–116 (Elsevier, Amsterdam, 2017).
- Bosmans, F. & Swartz, K. J. Targeting voltage sensors in sodium channels with spider toxins. *Trends Pharmacol. Sci.* **31**, 175–182 (2010).
- Wang, X. *et al.* Inhibitors of Ion Channels, Patent PCT/US2006/042882, 2006.
- Fulp, A., Marron, B., Suto, M., J. & Wang, X. Inhibitors of Voltage-Gated Sodium Channels, Patent PCT/US2006/031390, 2006.
- Kawatkar, A., S. *et al.* Bicyclic Derivatives as Modulators of Ion Channels, Patent PCT/US2006/017699, 2006.
- McCormack, K. *et al.* Voltage sensor interaction site for selective small molecule inhibitors of voltage-gated sodium channels. *Proc. Natl. Acad. Sci.* **110**, E2724–E2732 (2013).
- Zhang, M.-M. *et al.* Cooccupancy of the outer vestibule of voltage-gated sodium channels by micro-conotoxin KIIIA and saxitoxin or tetrodotoxin. *J. Neurophysiol.* **104**, 88–97 (2010).
- Shen, H. *et al.* Structural basis for the modulation of voltage-gated sodium channels by animal toxins. *Science* **362**, eaau2596 (2018).
- Ahuja, S. *et al.* Structural basis of Nav1.7 inhibition by an isoform-selective small-molecule antagonist. *Science* **350**, aac5464 (2015).
- Alexandrou, A. J. *et al.* Subtype-selective small molecule inhibitors reveal a fundamental role for Nav1.7 in nociceptor electrogenesis, axonal conduction and presynaptic release. *PLoS ONE* **11**, e0152405 (2016).
- Varney, M. Roche: At the Forefront of R&D Innovation and Breakthrough Treatments. [https://www.roche.com/dam/jcr:5c999124-c278-4549-8e94-4475cc741de1/en/2016\\_roche\\_cowen\\_presentation.pdf](https://www.roche.com/dam/jcr:5c999124-c278-4549-8e94-4475cc741de1/en/2016_roche_cowen_presentation.pdf) (2016)
- Schmalhofer, W. A. *et al.* ProTx-II, a selective inhibitor of Na<sub>v</sub>1.7 sodium channels, blocks action potential propagation in nociceptors. *Mol. Pharmacol.* **74**, 1476–1484 (2008).
- Xiao, Y. *et al.* Tarantula huwentoxin-IV inhibits neuronal sodium channels by binding to receptor site 4 and trapping the domain II voltage sensor in the closed configuration. *J. Biol. Chem.* **283**, 27300–27313 (2008).
- Deuis, J. R. *et al.* Pharmacological characterisation of the highly Na<sub>v</sub>1.7 selective spider venom peptide Pn3a. *Sci. Rep.* **7**, 40883 (2017).
- Moyer, B. D. *et al.* Pharmacological characterization of potent and selective Na<sub>v</sub>1.7 inhibitors engineered from *Chilobrachys jingzhao* tarantula venom peptide JzTx-V. *PLoS ONE* **13**, e0196791 (2018).
- Flinispach, M. *et al.* Insensitivity to pain induced by a potent selective closed-state Nav1.7 inhibitor. *Sci. Rep.* **7**, 39662 (2017).
- McKerrall, S. J. *et al.* Structure- and ligand-based discovery of chromane arylsulfonamide Nav1.7 inhibitors for the treatment of chronic pain. *J. Med. Chem.* **62**, 4091–4109 (2019).
- Graceffa, R. F. *et al.* Sulfonamides as selective Na<sub>v</sub>1.7 inhibitors: Optimizing potency, pharmacokinetics, and metabolic properties to obtain atropisomeric quinolinone (AM-0466) that affords robust in vivo activity. *J. Med. Chem.* **60**, 5990–6017 (2017).
- McDonnell, A. *et al.* Efficacy of the Nav1.7 blocker PF-05089771 in a randomised, placebo-controlled, double-blind clinical study in subjects with painful diabetic peripheral neuropathy. *Pain* **159**, 1465–1476 (2018).
- Rothenberg, M. E. *et al.* Safety, tolerability, and pharmacokinetics of GDC-0276, a novel Na<sub>v</sub>1.7 inhibitor, in a first-in-human, single- and multiple-dose study in healthy volunteers. *Clin. Drug Investig.* <https://doi.org/10.1007/s40261-019-00807-3> (2019).
- Walker, J. R. *et al.* Marked difference in saxitoxin and tetrodotoxin affinity for the human nociceptive voltage-gated sodium channel (Na<sub>v</sub>1.7). *Proc. Natl. Acad. Sci. USA* **109**, 18102–18107 (2012).
- Thomas-Tran, R. & Du Bois, J. Mutant cycle analysis with modified saxitoxins reveals specific interactions critical to attaining high-affinity inhibition of hNa<sub>v</sub>1.7. *Proc. Natl. Acad. Sci. USA* **113**, 5856–5861 (2016).

33. Tsukamoto, T. *et al.* Differential binding of tetrodotoxin and its derivatives to voltage-sensitive sodium channel subtypes (Nav1.1 to Nav1.7). *Br. J. Pharmacol.* **174**, 3881–3892 (2017).
34. Fleming, J. J., McReynolds, M. D. & Du Bois, J. (+)-saxitoxin: A first and second generation stereoselective synthesis. *J. Am. Chem. Soc.* **129**, 9964–9975 (2007).
35. Mulcahy, J. V., Walker, J. R., Merit, J. E., Whitehead, A. & Du Bois, J. Synthesis of the paralytic shellfish poisons (+)-gonyautoxin 2, (+)-Gonyautoxin 3, and (+)-11,11-dihydroxysaxitoxin. *J. Am. Chem. Soc.* **138**, 5994–6001 (2016).
36. Andresen, B. M. & Du Bois, J. De novo synthesis of modified saxitoxins for sodium ion channel study. *J. Am. Chem. Soc.* **131**, 12524–12525 (2009).
37. Walker, J. R., Merit, J. E., Thomas-Tran, R., Tang, D. T. Y. & Du Bois, J. Divergent synthesis of natural derivatives of (+)-saxitoxin including 11-saxitoxinethanoic acid. *Angew. Chem. Int. Ed. Engl.* **58**, 1689–1693 (2019).
38. Lipkind, G. M. & Fozzard, H. A. A structural model of the tetrodotoxin and saxitoxin binding site of the Na<sup>+</sup> channel. *Biophys. J.* **66**, 1–13 (1994).
39. Penzotti, J. L., Fozzard, H. A., Lipkind, G. M. & Dudley, S. C. Differences in saxitoxin and tetrodotoxin binding revealed by mutagenesis of the Na<sup>+</sup> channel outer vestibule. *Biophys. J.* **75**, 2647–2657 (1998).
40. Tikhonov, D. B. & Zhorov, B. S. Modeling P-loops domain of sodium channel: Homology with potassium channels and interaction with ligands. *Biophys. J.* **88**, 184–197 (2005).
41. Shen, H., Liu, D., Wu, K., Lei, J. & Yan, N. Structures of human Nav<sub>v</sub>1.7 channel in complex with auxiliary subunits and animal toxins. *Science* **363**, 1303–1308 (2019).
42. Goral, R. O., Leipold, E., Nematian-Ardestani, E. & Heinemann, S. H. Heterologous expression of Nav<sub>v</sub>1.9 chimeras in various cell systems. *Pflugers Arch.* **467**, 2423–2435 (2015).
43. Satin, J. *et al.* A mutant of TTX-resistant cardiac sodium channels with TTX-sensitive properties. *Science* **256**, 1202–1205 (1992).
44. Gingras, J. *et al.* Global Nav1.7 knockout mice recapitulate the phenotype of human congenital indifference to pain. *PLoS ONE* **9**, e105895 (2014).
45. Shields, S. D. *et al.* Insensitivity to pain upon adult-onset deletion of Nav1.7 or its blockade with selective inhibitors. *J. Neurosci.* **38**, 10180–10201 (2018).
46. Minett, M. S. *et al.* Distinct Nav1.7-dependent pain sensations require different sets of sensory and sympathetic neurons. *Nat. Commun.* **3**, 791 (2012).
47. Yeomans, D. C. *et al.* Recombinant herpes vector-mediated analgesia in a primate model of hyperalgesia. *Mol. Ther.* **13**, 589–597 (2006).
48. Cooper, B. Y., Vierck, C. J. & Yeomans, D. C. Selective reduction of second pain sensations by systemic morphine in humans. *Pain* **24**, 93–116 (1986).
49. Tzabazis, A. Z. *et al.* Selective nociceptor activation in volunteers by infrared diode laser. *Mol. Pain* **7**, 18 (2011).
50. Yeomans, D. C., Pirec, V. & Proudfit, H. K. Nociceptive responses to high and low rates of noxious cutaneous heating are mediated by different nociceptors in the rat: behavioral evidence. *Pain* **68**, 133–140 (1996).
51. Loggia, M. L., Juneau, M. & Bushnell, C. M. Autonomic responses to heat pain: Heart rate, skin conductance, and their relation to verbal ratings and stimulus intensity. *Pain* **152**, 592–598 (2011).
52. Theile, J. W., Fuller, M. D. & Chapman, M. L. The selective Nav1.7 inhibitor, PF-05089771, interacts equivalently with fast and slow inactivated Nav1.7 channels. *Mol. Pharmacol.* **90**, 540–548 (2016).
53. Alles, S. R. A. *et al.* Sensory neuron-derived Nav<sub>v</sub>1.7 contributes to dorsal horn neuron excitability. *Sci. Adv.* **6**, eaax4568 (2020).

## Acknowledgements

Research reported in this publication was supported in part (60%) by an award to SiteOne Therapeutics from the National Institute of Neurological Disorders and Stroke of the National Institutes of Health under award number R44NS081887 and by the National Institutes of Health R01 GM117263-01A1 (JDB). HSH is supported by the Department of Defense (DoD) through the National Defense Science & Engineering Graduate (NDSEG) Fellowship Program and is a fellow of the Center for Molecular Analysis and Design (CMAD) at Stanford University. The content is solely the responsibility of the authors and does not necessarily represent the official views of the National Institutes of Health. Christine O'Rourke, DVM, DACLAM and the Montana State Animal Resource Center are gratefully acknowledged for assistance with animal studies.

## Author contributions

J.V.M., J.D.B., D.C.Y., H.P., and A.D. conceived of the study. H.P., J.T.B., A.D., H.S.H., G.L., D.M., X.Z., J.L., S.A., B.D.M., D.C.Y. and J.V.M. designed and performed experiments. J.T.B. and J.V.M. drafted the manuscript. J.D.B., D.C.Y., A.D. and B.D.M. critically revised the manuscript. All authors reviewed and approved the manuscript.

## Competing interests

H.P., J.T.B., A.D., G.L., D.M., X.Z. and J.V.M. are employees of and shareholders in SiteOne Therapeutics. D.C.Y. and J.D.B. are advisors to and shareholders in SiteOne Therapeutics.

## Additional information

**Supplementary information** is available for this paper at <https://doi.org/10.1038/s41598-020-71135-2>.

**Correspondence** and requests for materials should be addressed to J.V.M.

**Reprints and permissions information** is available at [www.nature.com/reprints](http://www.nature.com/reprints).

**Publisher's note** Springer Nature remains neutral with regard to jurisdictional claims in published maps and institutional affiliations.





**Open Access** This article is licensed under a Creative Commons Attribution 4.0 International License, which permits use, sharing, adaptation, distribution and reproduction in any medium or format, as long as you give appropriate credit to the original author(s) and the source, provide a link to the Creative Commons licence, and indicate if changes were made. The images or other third party material in this article are included in the article's Creative Commons licence, unless indicated otherwise in a credit line to the material. If material is not included in the article's Creative Commons licence and your intended use is not permitted by statutory regulation or exceeds the permitted use, you will need to obtain permission directly from the copyright holder. To view a copy of this licence, visit <http://creativecommons.org/licenses/by/4.0/>.

© The Author(s) 2020